

User-defined, temporal presentation of bioactive molecules on hydrogel substrates using supramolecular coiled-coil complexes

M. Gregory Grewal^a, Vincent P. Gray^a, Rachel A. Letteri^a, and Christopher B. Highley^{a,b,*}

^a Department of Chemical Engineering, University of Virginia, Charlottesville, VA

^b Department of Biomedical Engineering, University of Virginia, Charlottesville, VA

Table of Contents

Section I. Primary structure characterization of polymers and peptides

Figure S1. Norbornene-functionalized hyaluronic acid (NorHA) ¹H NMR spectrum

Table S1. Mass spectrometry of peptides used in this study

Figure S2. Electrospray ionization (ESI) mass spectra for coiled-coil peptides

Figure S3. ESI spectrum for thiolated fluorophore peptide used for covalent controls in this study

Figure S4. HPLC traces for peptides used in this study

Section II. Secondary structure characterization

Figure S5. Circular dichroism (CD) spectra for coiled peptides used in this study

Table S2. α -helix percentage for peptides used in this study

Section III. Characterization of intermolecular interactions

Figure S6. ITC runs of T-Peptide:Coiled-RGD Peptide association in NIH 3T3 fibroblast medium

Figure S7. ITC runs of Coiled-RGD Peptide:D-Peptide association in NIH 3T3 fibroblast medium

Figure S8. ITC runs of T-Peptide:D-Peptide association in NIH 3T3 fibroblast medium

Figure S9. ITC runs of T-Peptide:A-Peptide association in PBS

Figure S10. ITC runs of T-Peptide:Coiled-RGD Peptide associations in PBS

Figure S11. ITC runs of A-Peptide:D-Peptide associations in PBS

Figure S12. ITC runs of Coiled-RGD Peptide:D-Peptide associations in PBS

Figure S13. ITC runs of T-Peptide:D-Peptide associations in PBS

Figure S14. Concentration dependency of D-peptide on release of A-peptide with comparison to release in cell media

Section IV. References

I. Primary structure characterization of polymers and peptides

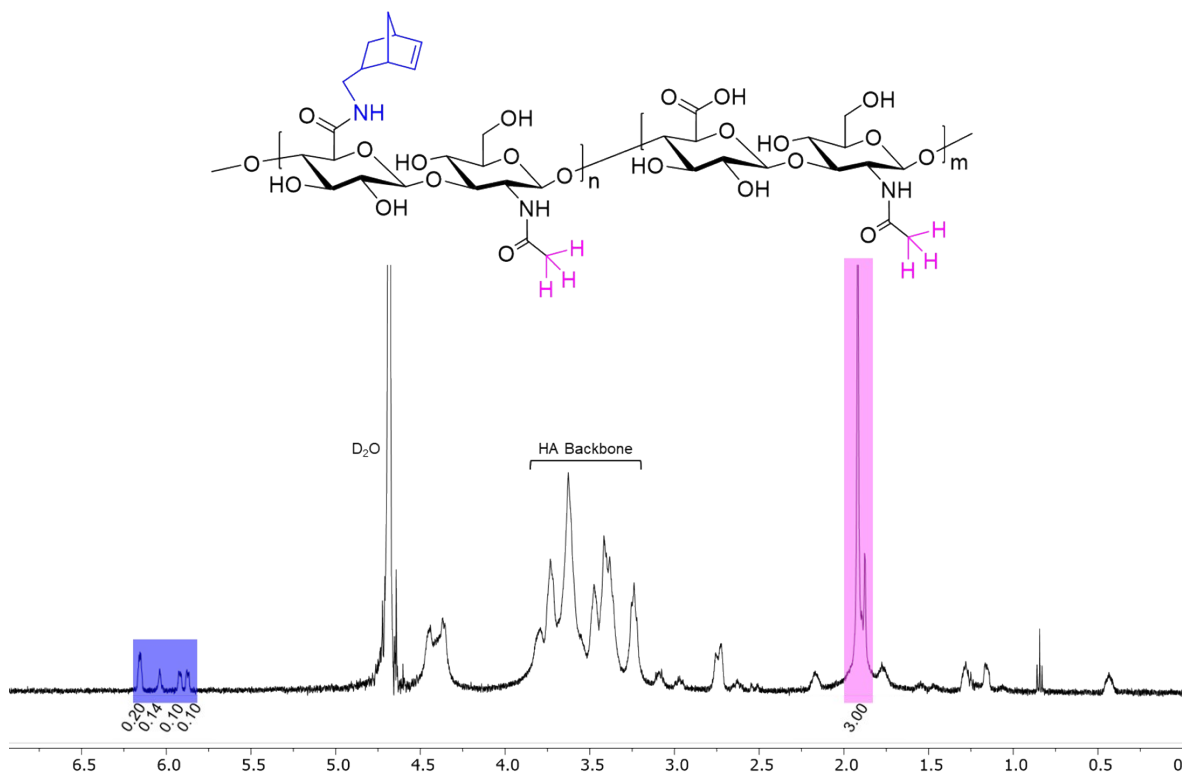


Figure S1. Norbornene-functionalized hyaluronic acid (NorHA) ^1H NMR spectrum. Spectrum is normalized to a value of 3.00 based on the methyl groups highlighted in pink, and degree of functionalization was determined based on the integral values associated with the norbornene groups (endo- and exo-) highlighted in blue. Degree of HA modification with norbornene groups was determined to be $\sim 25\%$.

Table S1. Mass spectrometry of peptides used in this study. Peptide sequences, with corresponding text nomenclature, along with their calculated and observed m/z values as determined by electrospray ionization (ESI) mass spectroscopy. Refer to Figures S2 and S3 for spectra.

Sequence	Peptide Title	Calculated m/z	Observed m/z
$\text{H}_2\text{N}-(\text{EIAALEK})_3\text{G}_7\text{CG-NH}_2$	T-peptide	2839.47	2840.47
$\text{H}_2\text{N-FAM}-(\text{KIAALKE})_4\text{-NH}_2$	A-peptide	3389.24	3390.96
$\text{H}_2\text{N-GYGRGDSPG}-(\text{KIAALKE})_4\text{-NH}_2$	Coiled RGD	3877.29	3879.28
$\text{H}_2\text{N}-(\text{EIAALEK})_4\text{-NH}_2$	D-Peptide	3034.71	3035.71
$\text{H}_2\text{N-FAM}-(\text{EIAALEK})_3\text{-G}_3\text{-CG-NH}_2$	Covalent	2969.70	2970.43

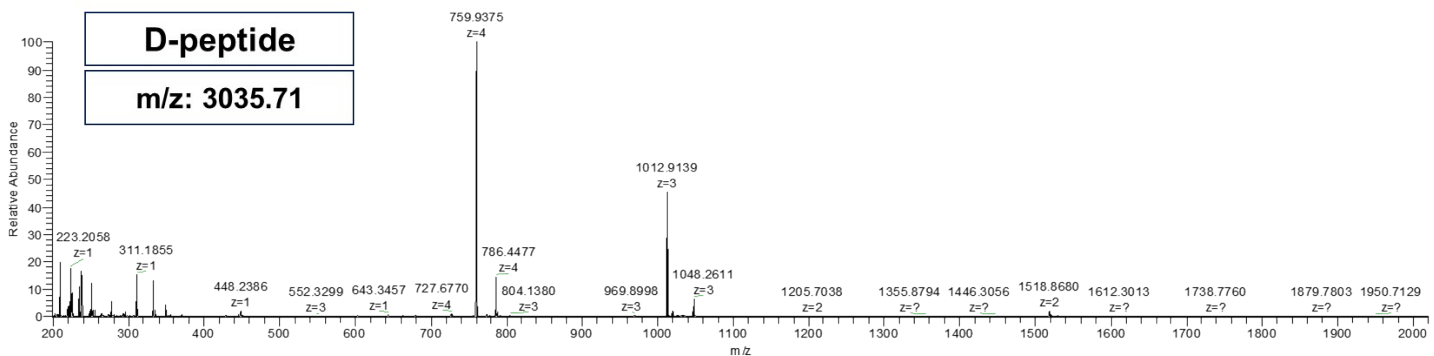
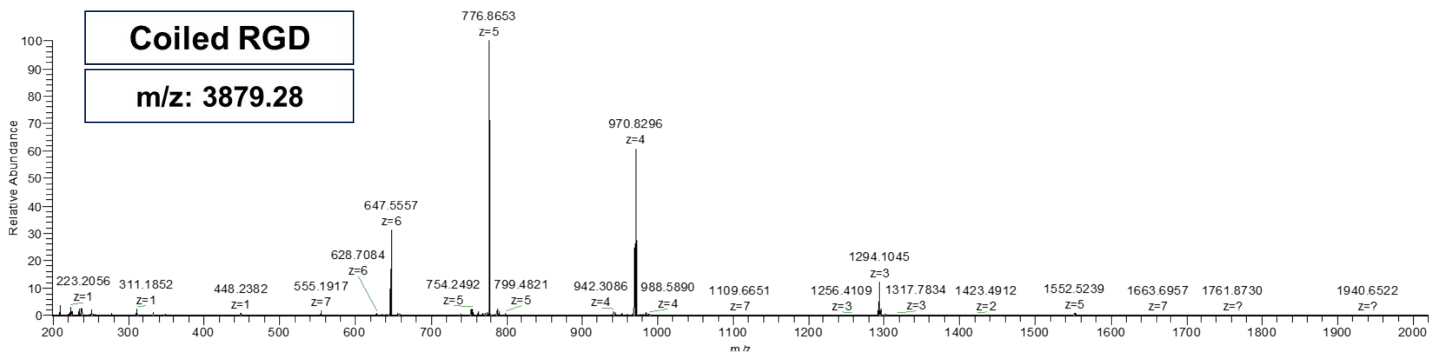
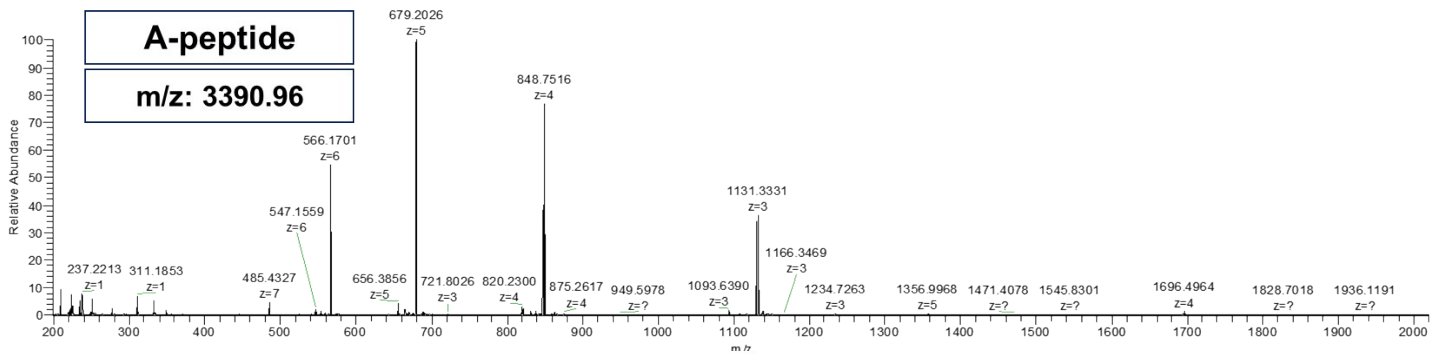
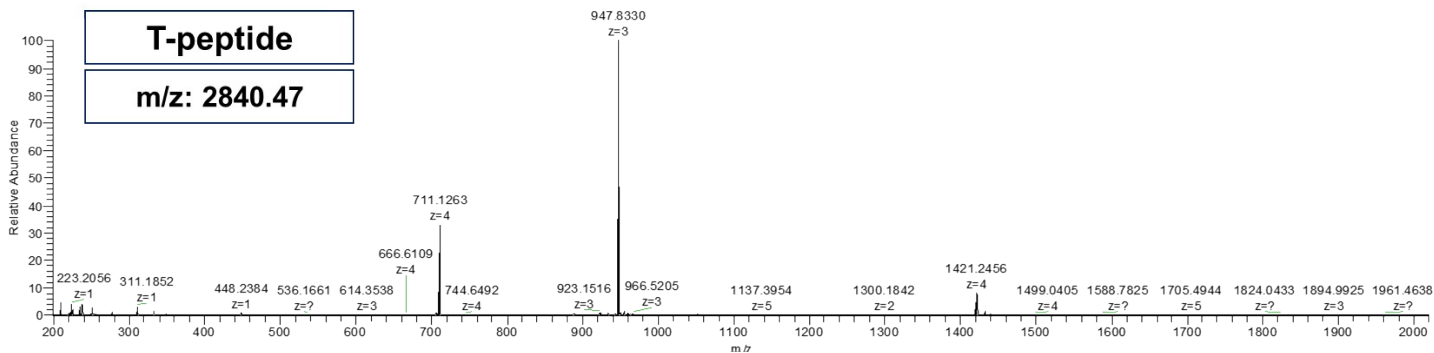


Figure S2. Electrospray ionization (ESI) mass spectra for coiled-coil peptides. Refer to Table S1 for calculated and observed m/z.

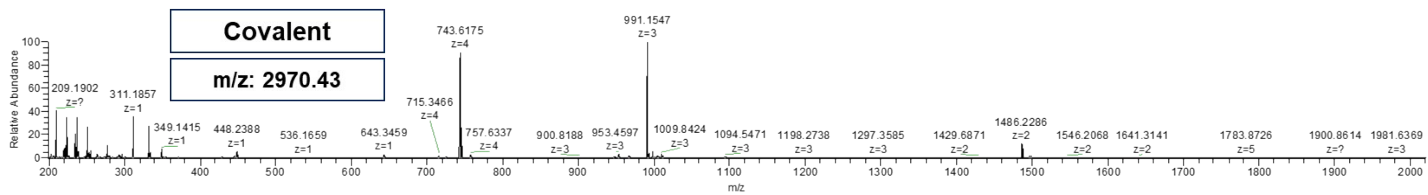


Figure S3. ESI spectrum for thiolated fluorophore peptide used for covalent controls in this study. Refer to Table S1 for calculated and observed m/z . It is important to note that although this was the observed m/z value, there were non-negligible amounts of other molecular weights in this peptide – likely partially from N-termini without conjugated FAM and disulfide bridges forming.

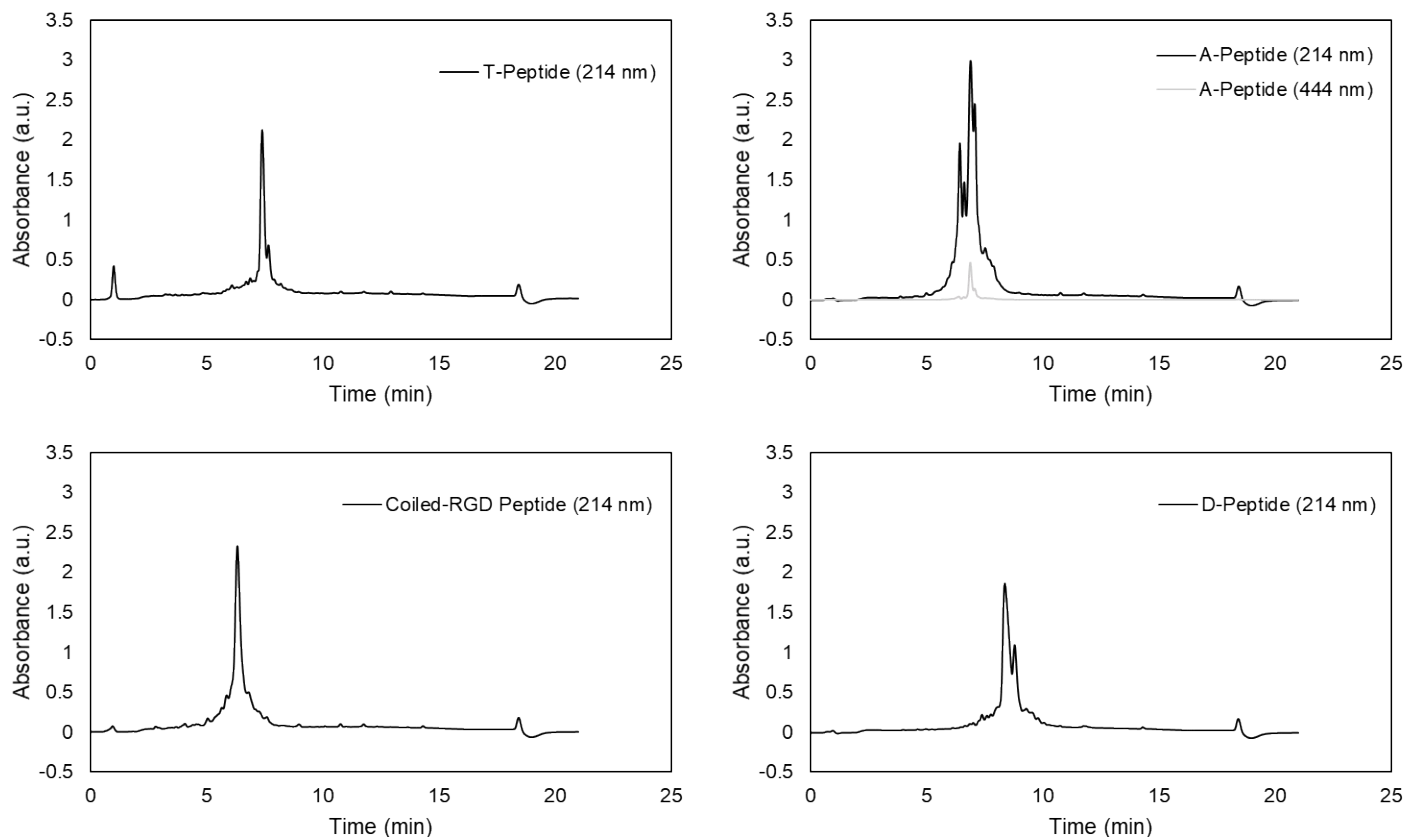


Figure S4. Analytical HPLC traces for peptides used in this study. Synthetic peptides were detected at 214 nm, while FAM absorbance on the A-peptide was detected at 444 nm. The 444 nm trace for the A-peptide confirms that one peak in the chromatograph corresponds to labeled peptide, suggesting that the other corresponds to unlabeled peptide. Peptides were eluted using an AB linear gradient of 6.2% $\text{CH}_3\text{CN}/\text{min}$ from 5 to 95% CH_3CN , where eluent A was 0.1% aqueous trifluoroacetic acid (v/v) and eluent B was 0.1% trifluoroacetic acid in CH_3CN .

II. Secondary structure characterization

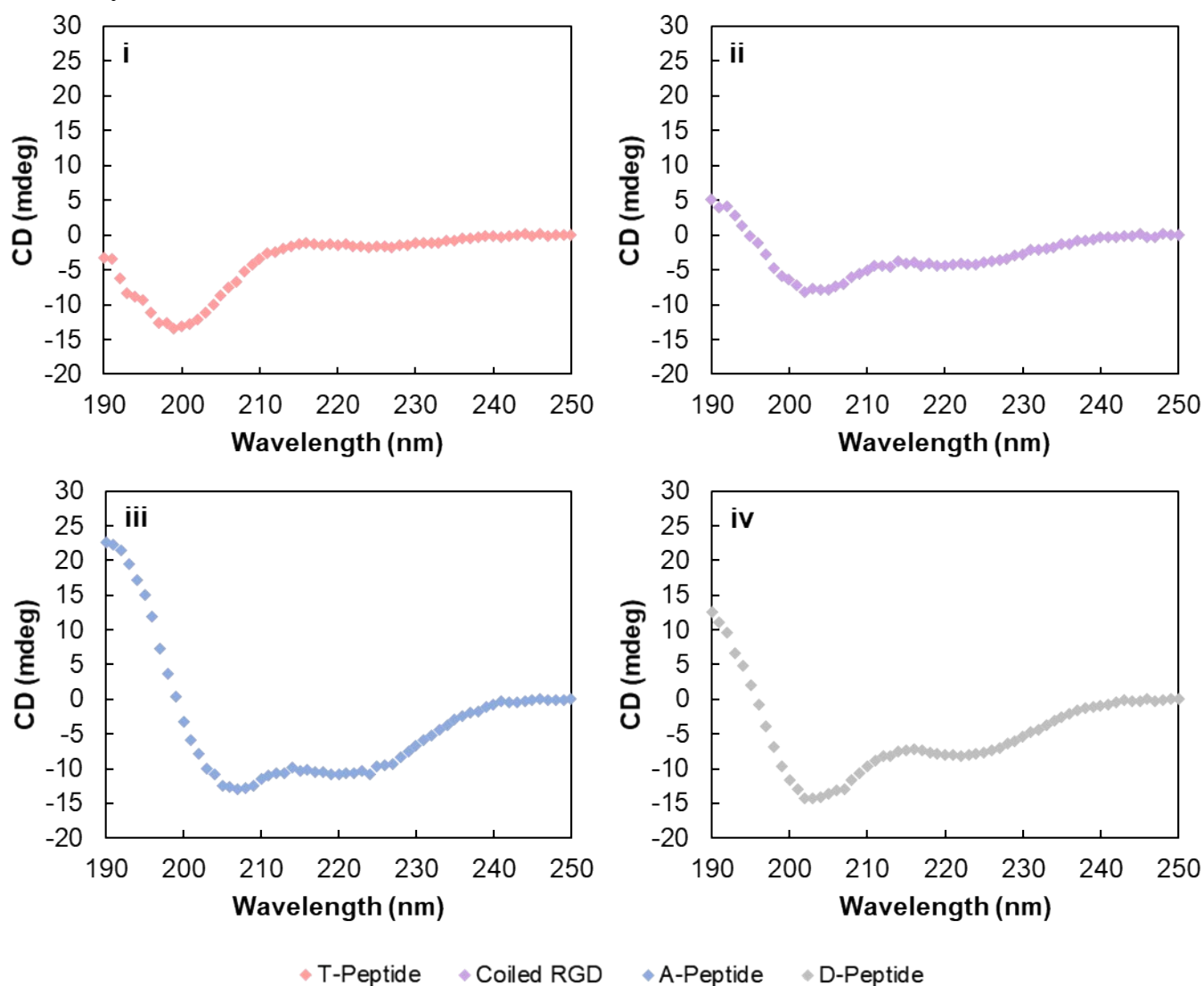


Figure S5. Circular dichroism (CD) spectra of coiled coil-forming peptides used in this study. CD spectra of (i) T-peptide, (ii) Coiled RGD, (iii) A-peptide, and (iv) D-peptide in 10 mM PBS (pH 7.4) at 0.1 mg/mL. CD measurements were taken at 25 °C, with a data pitch of 0.1 nm and scanning speed of 50 nm/min. The spectra are shown as the average of 3 scans per sample.

Table S2. α -helix percentage for peptides used in this study. Helicity calculations were performed based on a previously described method.¹

Peptide Title	Percent Helicity
T-peptide	4.6%
Coiled RGD	10.8%
A-peptide	29.1%
D-Peptide	22.6%

The spectrum of the T-peptide (EIAALEK)₃G₇CG (S4-i) shows the peptide adopts a random coil structure (overall α -helicity of 4.6%). As the T-peptide behaved how we expected it to in forming coiled-coil complexes with release being dependent on the addition of the competing D-peptide (see publication Figure 2), we postulate that the 7-glycine spacer added to provide physical space between the hydrogel/fiber substrates and the coiled domains might also consequently limit the overall α -helical nature of the peptide. That said, it still allowed for stable

coiled-coil complexes to form on hydrogel/hydrogel fiber substrates that could easily be disrupted via the user-defined addition of the complementary D-peptide. This was unsurprising as randomly coiled peptides have been previously shown to adopt the helical secondary structure as they assemble into coiled-coil complexes – specifically when the sequence contains the necessary amino acid motifs to complex with the complementary strand as they do here (E/K complementary heptads)².

The spectrum of the Coiled RGD peptide GYGRGDSPG-(KIAALKE)₄ (S4-ii) shows a modest helical structure based on the CD spectrum (overall α -helicity of 10.8%), with the addition of the bioactive RGD domain likely limiting the formation of the α -helix – as (KIAALKE)₄ itself has been previously shown to be α -helical³.

The A-peptide (S4-iii) – FAM-(KIAALKE)₄ – and the D-peptide (S4-iv) – (EIAALEK)₄ – have the highest α -helical content among the peptides in this study (overall α -helicity of 29.1% and 22.6%, respectively), as indicated by the CD spectra. Overall, despite the peptides exhibiting varying degrees of α -helicity, they demonstrated the ability to form coiled-coil complexes with their complements, thus enabling user-defined, temporal presentation of bioactive molecules on NorHA hydrogels and PEG-NB fibers as shown in Figures 1 and 2 (fluorophore experiments), as well as Figures 3 and 4 (fibroblast experiments).

Section III. Characterization of intermolecular interactions

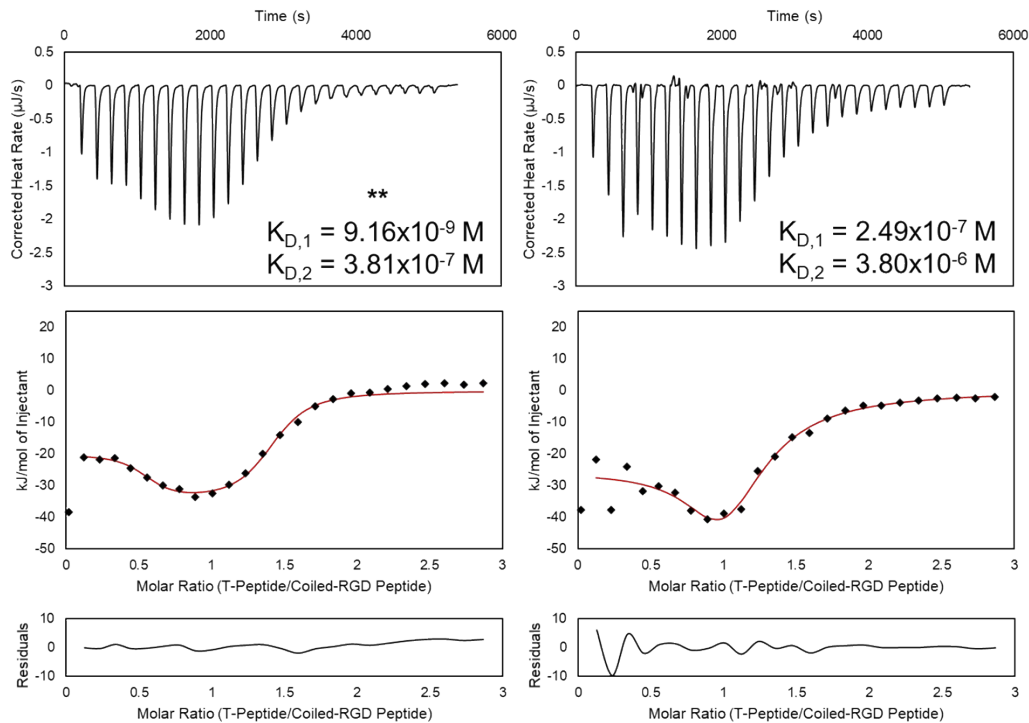


Figure S6. ITC trials for T-Peptide:Coiled-RGD Peptide associations in NIH 3T3 fibroblast medium. Experiments were performed with injections of 200 μM T-Peptide into 20 μM Coiled-RGD Peptide at pH 7.4. Integrated plots were fit to a multiple-site model that yielded affinity parameters for these complexes. T-Peptide:Coiled-RGD Peptide dissociation constant values from the model are on the order of 10^{-7} - 10^{-9} M for the first site and 10^{-6} - 10^{-7} M for the second site. ** Indicates plot series included in main text Figure 1.

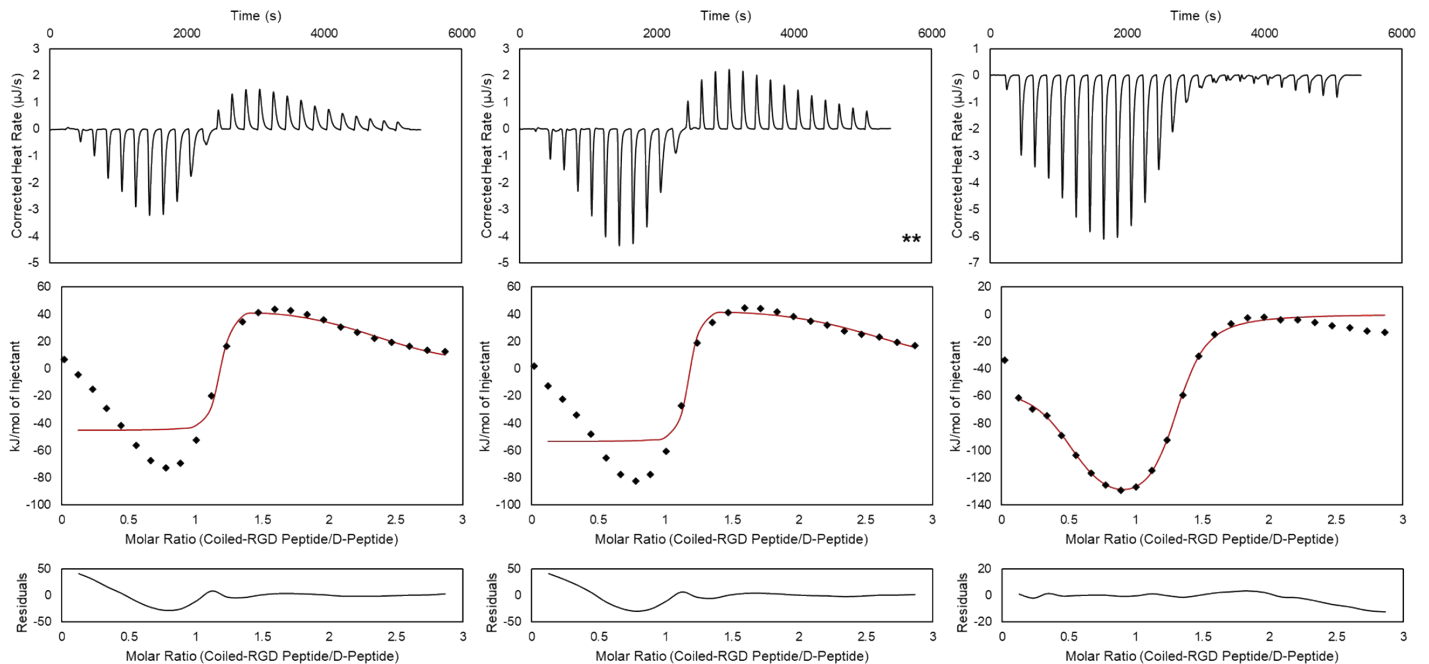


Figure S7. ITC Trials for Coiled-RGD Peptide:D-Peptide associations in NIH 3T3 fibroblast medium. Experiments were performed with injections of 200 μM Coiled-RGD Peptide into 20 μM D-Peptide at pH 7.4. Integrated plots were fit to a multiple-site model that yielded affinity information for these complexes; however,

the plots (notably left and middle) demonstrated high residuals for the fits at low molar ratios, indicating that the models may not reliably represent the data. Therefore, K_D values from the model would not accurately represent the system. Nevertheless, the magnitudes of the exothermic peaks (refer to y-axes on integrated plots) are considerably greater than those seen for T-Peptide:Coiled RGD Peptide (Figure S6), indicating that the Coiled-RGD:D-Peptide complex is thermodynamically favored compared to the T-Peptide:Coiled-RGD Peptide complex in culture medium. This favorability likely facilitates the removal of Coiled-RGD peptide from T-Peptide via the introduction of D-peptide into the system. Notably, the ITC traces exhibit endothermic peaks (left and middle), which are potentially indicative of higher-order structures forming in solution⁴. Interestingly, the last plot series (right) does not exhibit the endothermic peaks seen in the other two traces, and we are currently investigating the cause of the endothermic peaks as a separate study. **** Indicates plot series included in main text Figure 1.**

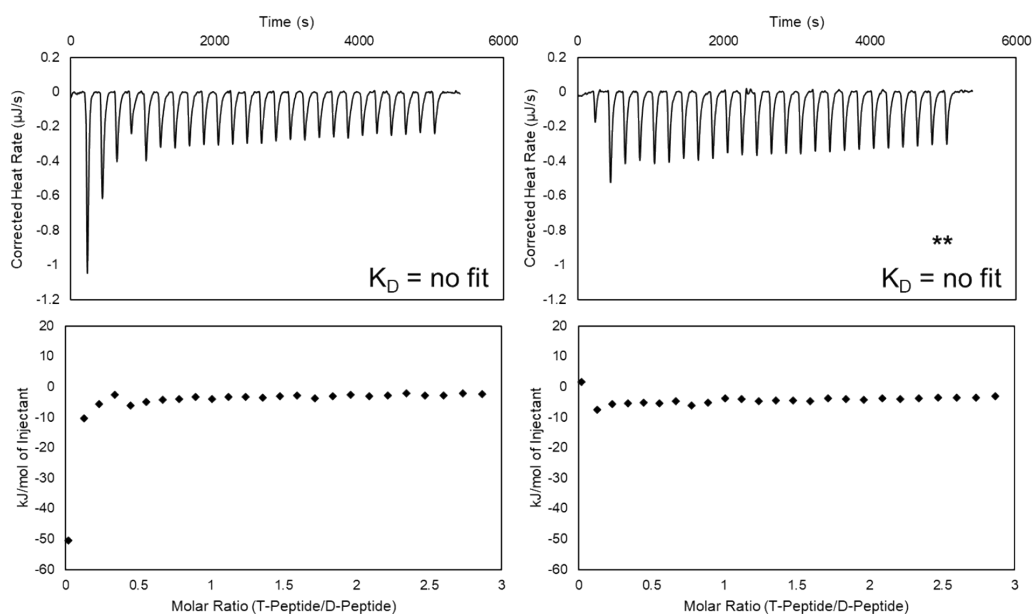


Figure S8. ITC trials for T-Peptide:D-Peptide associations in NIH 3T3 fibroblast medium. Experiments were performed with injections of 200 μ M T-Peptide into 20 μ M D-Peptide at pH 7.4. Integrated plots were unable to be fit to an association model and subtracting integrated heats of dilution yield heats of interaction of essentially 0 kJ/mol. Therefore, the T-Peptide and D-peptide do not appreciably associate when in fibroblast culture medium. **** Indicates plot series included in main text Figure 1.**

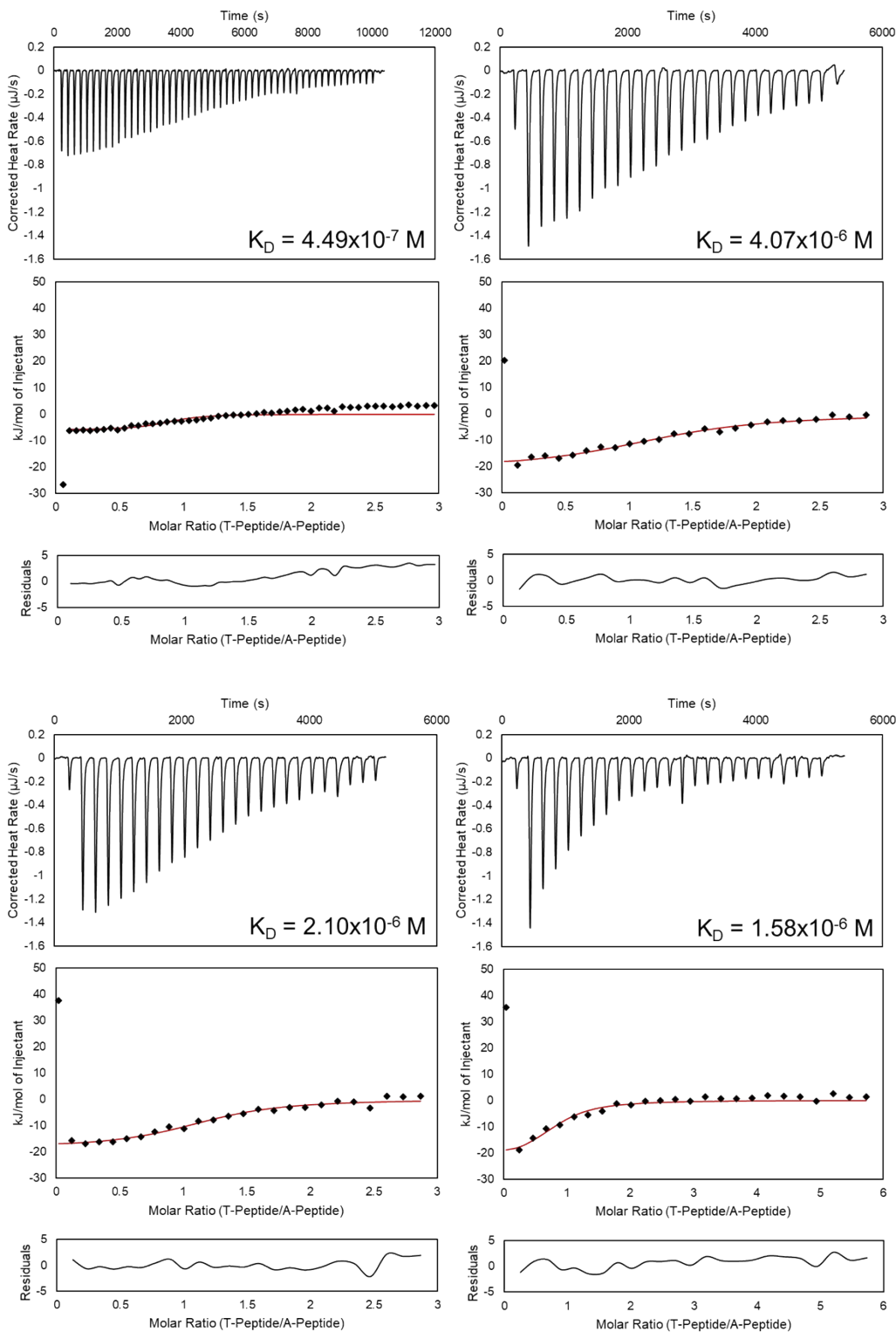


Figure S9. ITC trials for T-Peptide:A-Peptide associations in PBS. Experiments were performed with injections of $200 \mu\text{M}$ T-Peptide into $20 \mu\text{M}$ A-Peptide at pH 7.4, with the exception of the final trace (bottom right), which was performed with injections of $200 \mu\text{M}$ T-Peptide into $10 \mu\text{M}$ A-Peptide at pH 7.4. The first trace (top left) was performed with 50 injections, whereas the remaining traces were performed with 25 injections. Integrated plots were fit to an independent-site model that yielded affinity parameters for these complexes. T-Peptide:A-Peptide dissociation constant values are on the order of 10^{-6} - 10^{-7} M .

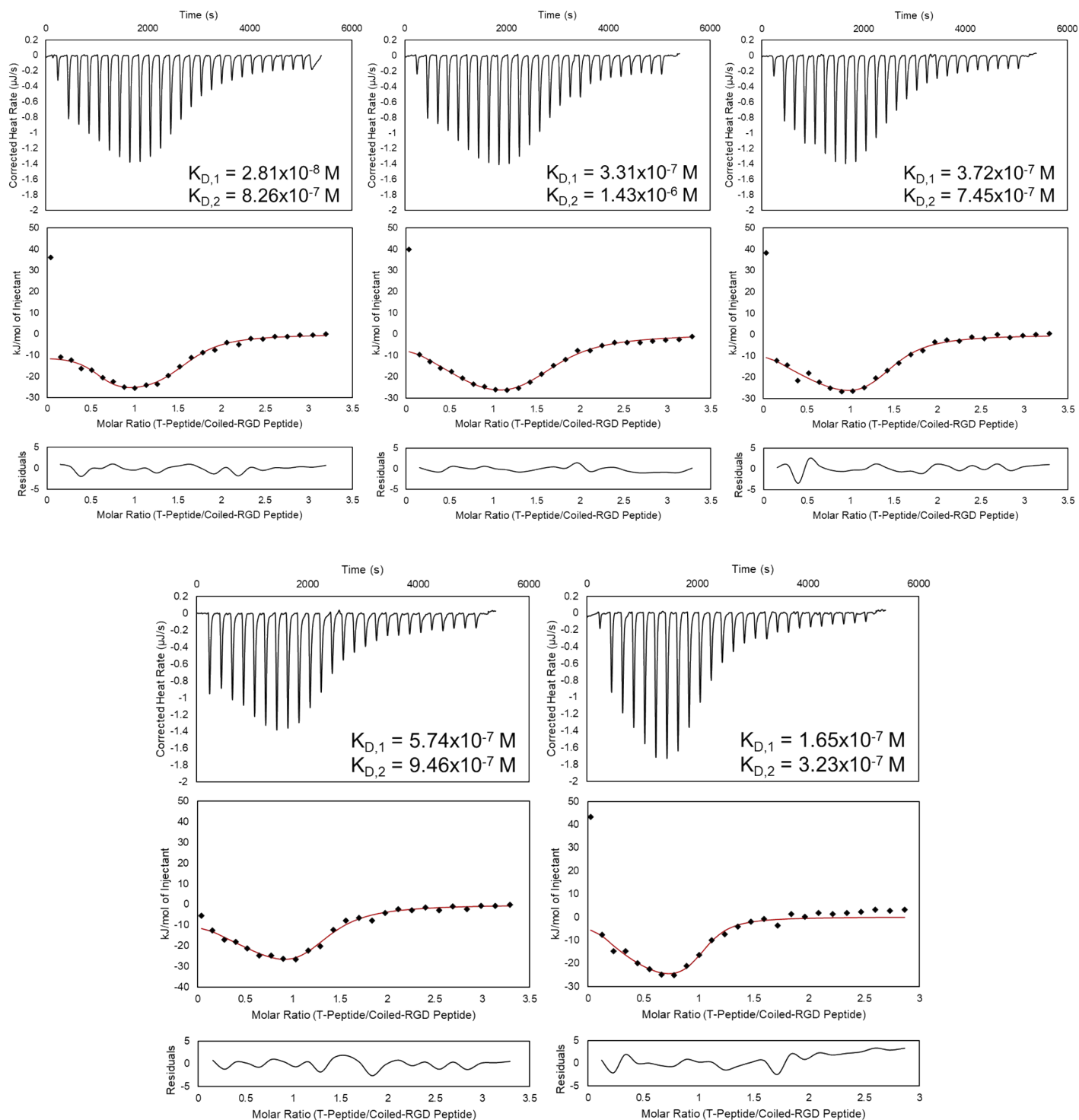


Figure S10. ITC trials for T-Peptide:Coiled-RGD Peptide associations in PBS. Experiments were performed with injections of 172 μM T-Peptide into 16 μM Coiled-RGD Peptide at pH 7.4, with the exception of the final trace (bottom right), which was performed with injections of 200 μM T-Peptide into 20 μM Coiled-RGD Peptide at pH 7.4. Integrated plots were fit to a multiple-site model that yielded affinity parameters for these complexes. T-Peptide:Coiled-RGD Peptide dissociation constant values are on the order of 10^{-7} - 10^{-8} M for the first site and 10^{-6} - 10^{-7} M for the second site.

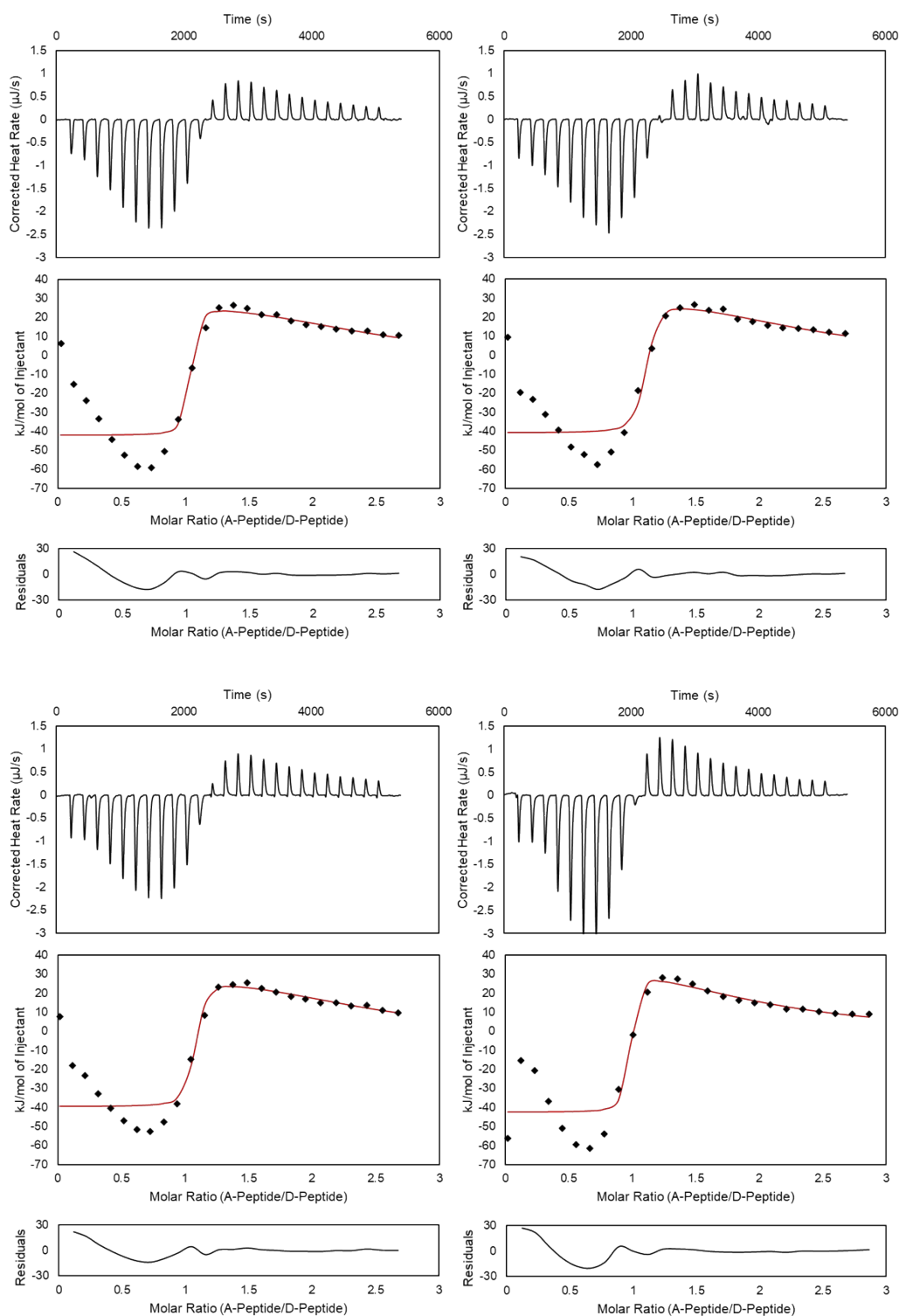


Figure S11. ITC trials for A-Peptide:D-Peptide associations in PBS. Experiments were performed with injections of 155 μM A-Peptide into 17 μM D-Peptide at pH 7.4, with the exception of the final trace (bottom right), which was performed with injections of 200 μM A-Peptide into 20 μM D-Peptide at pH 7.4. Integrated plots were fit to a multiple-site model that yielded affinity information for these complexes; however, the plots all demonstrated high residuals for the fits at low molar ratios, indicating that the models may not reliably represent the data. Therefore, K_D values from the model would not accurately represent the system. Nevertheless, the magnitudes of the exothermic peaks (refer to y-axes on integrated plots) are considerably greater than those

seen for T-Peptide:A-Peptide (Figure S9), indicating that the A-Peptide:D-Peptide complex is thermodynamically favorable compared to the T-Peptide:A-Peptide in PBS. This favorability likely facilitates the removal of A-peptide from T-Peptide via the introduction of D-peptide into the system. Notably, the ITC traces exhibit endothermic peaks, which are potentially indicative of higher-order structures forming in solution⁴.

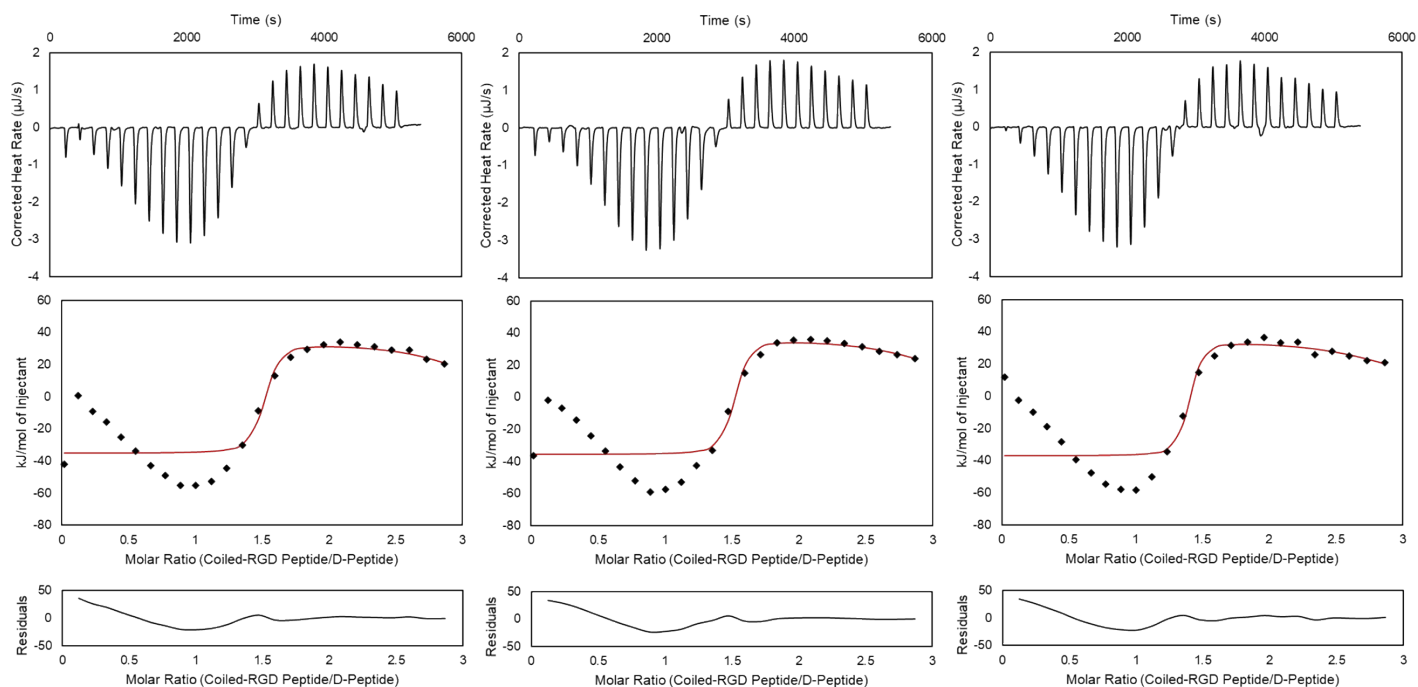


Figure S12. ITC trials for Coiled-RGD Peptide:D-Peptide associations in PBS. Experiments were performed with injections of 200 μM Coiled-RGD Peptide into 20 μM D-Peptide at pH 7.4. Integrated plots were fit to a multiple-site model that yielded affinity information for these complexes; however, the plots all demonstrated high residuals for the fits, indicating that the models may not reliably represent the data. Therefore, K_D values from the model would not accurately represent the system. Nevertheless, the magnitudes of the exothermic peaks (refer to y-axes on integrated plots) are considerably greater than those seen for T-Peptide:Coiled-RGD Peptide (Figure S10), indicating that the Coiled-RGD Peptide:D-Peptide complex is thermodynamically favorable compared to the T-Peptide:Coiled-RGD Peptide in PBS. This favorability likely facilitates the removal of Coiled-RGD peptide from T-Peptide via the introduction of D-peptide into the system. Notably, the ITC traces exhibit endothermic peaks, which are potentially indicative of higher-order structures forming in solution⁴.

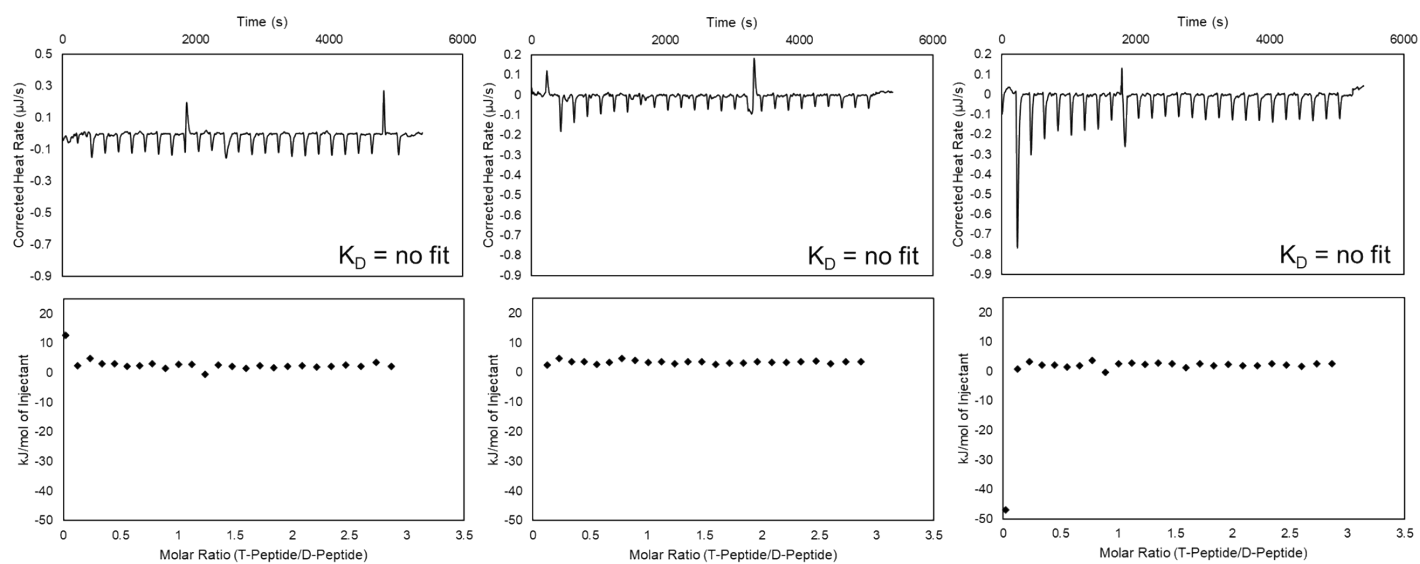


Figure S13. ITC trials for T-Peptide:D-Peptide associations in PBS. Experiments were performed with injections of 200 μM T-Peptide into 20 μM D-Peptide at pH 7.4. Integrated plots were unable to be fit to an association model and subtracting integrated heats of dilution yield heats of interaction of essentially 0 kJ/mol. Therefore, the T-Peptide and D-peptide do not appreciably associate in PBS.

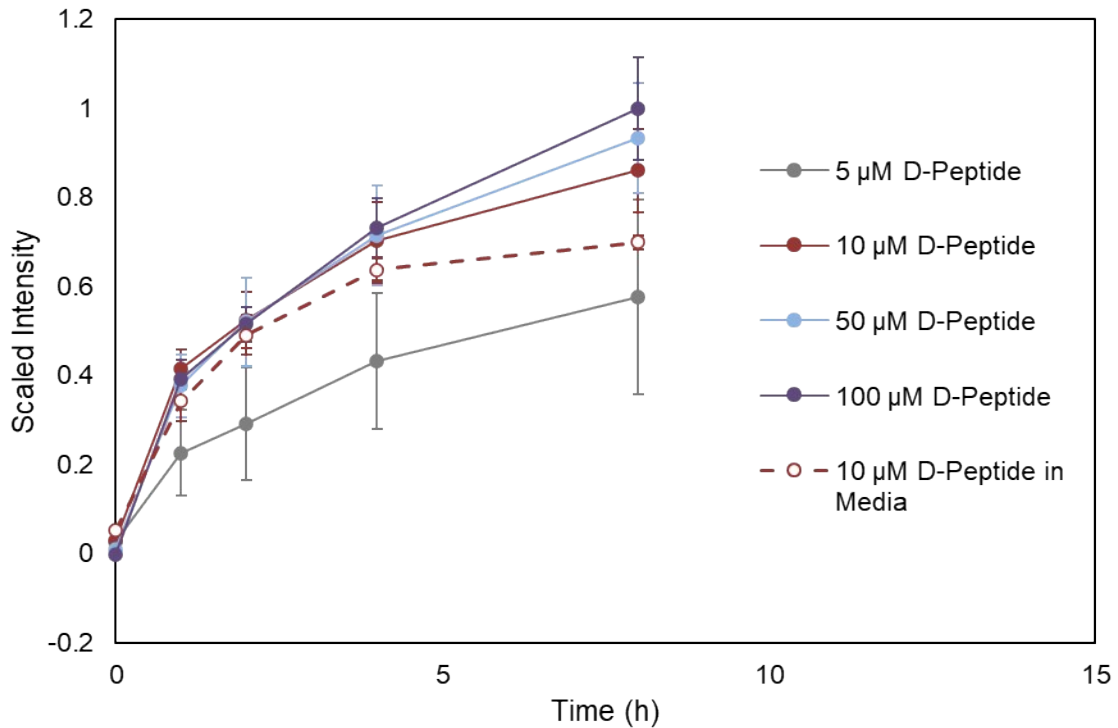


Figure S14. Concentration dependency of D-peptide on release of A-peptide with comparison to release in cell media. Release of A-Peptide with 5, 10, 50, and 100 μM D-Peptide solutions *in PBS* illustrates that increasing concentration of D-Peptide increases removal of A-peptide from the system. However, at higher concentrations, only marginal improvement is observed in A-peptide removal – suggesting that kinetics of peptide displacement govern removal rather than D-Peptide availability at higher concentrations.

10 μM D-peptide *in 3T3 fibroblast media* generally follows the same trend with marginally lower removal compared to 10 μM D-Peptide in PBS. This could be due to interactions with the serum in media, but it is more likely that differences in FAM concentration in cell media are more difficult to track with the plate reader protocol. We refer to the ITC data (Figures S6-13) that indicate similar affinities in both PBS and cell media.

IV. References:

- 1 B. Forood, E. J. Feliciano and K. P. Nambiar, *Proc. Natl. Acad. Sci.*, 1993, **90**, 838–842.
- 2 B. Apostolovic and H. A. Klok, *Biomacromolecules*, 2008, **9**, 3173–3180.
- 3 J. R. Litowski and R. S. Hodges, *J. Biol. Chem.*, 2002, **277**, 37272–37279.
- 4 M. Kabiri, I. Bushnak, M. T. McDermot and L. D. Unsworth, *Biomacromolecules*, 2013, **14**, 3943–3950.